Exp Brain Res (1998) 121:76–91

RESEARCH ARTICLE

Ian E. Brown · Takahiro Satoda
Frances J.R. Richmond · Gerald E. Loeb

Feline caudofemoralis muscle

Muscle fibre properties, architecture, and motor innervation

Received: 22 September 1997 / Accepted: 29 December 1997

Abstract Feline caudofemoralis (CF) is a promising preparation in which to study the properties of mammalian fast-twitch skeletal muscle, but little is known about its muscle fiber properties, architecture, and motor innervation. We used histochemical techniques to confirm that it contained predominantly type IIB fibers (95±2%, n=8, with six of eight muscles composed exclusively of type IIA and IIB fibers), but physiological experiments showed less fatiguability than for the type IIB component of medial gastrocnemius. This may be related to the surprisingly strong and regular recruitment of CF during repetitive tasks such as walking and trotting, which we demonstrated electromyographically. We measured muscle length over the anatomical range of motion for CF (∼0.6–1.2 L_0) and estimated working length during walking and trotting (∼0.95–1.15 L_0). The specific tension was similar to that of the exclusively slow-twitch soleus muscle (31.2±4.7 N/cm^2 compared with 31.8±4.1 N/cm^2; P>0.8). Single fiber dissections of CF revealed a series-fibered architecture with a mean of 2.3 fibers, each 2.5 cm long, required to span the fascicle length. We identified two neuromuscular compartments in CF by cutting one of the two nerve branches innervating CF and depleting the glycogen stores in the intact motor units. These compartments were in parallel and extended the length of the muscle; their electromyographic activity was similar during various natural behaviors. CF and gluteus maximus motoneurons were labeled concurrently with a combination of fluorescent, retrograde tracers including Fluororuby, Fluorogold and Fast Blue. The CF motor nucleus was located in L7-S1, overlapping and intermingling extensively with the nucleus of the adjacent gluteus maximus muscle. Distributions of CF motoneuron diameter revealed one large peak around 50–55 μm, with relatively few small-diameter (less than 35 μm) cells. Using estimates of the total number of fibers in three muscles and the estimated number of α-motoneurons for those same muscles, we calculated a mean innervation ratio of ∼270, which is at the low end of the innervation ratios for type IIB motor units from other feline muscles and more similar to type IIA motor units. In general, CF appears to be a useful preparation in which to study the properties of fast-twitch muscle, but these properties may vary somewhat from type IIB fibers from different muscles.

Key words Motor nucleus · EMG · Muscle architecture · Muscle fiber · Caudofemoralis · Cat

I.E. Brown · T. Satoda[1] · F.J.R. Richmond · G.E. Loeb
MRC Group in Sensory-Motor Neuroscience
and the Department of Physiology, Queen's University,
Kingston, Ontario, K7L 3N6, Canada

G.E. Loeb (✉)
Bio-Medical Engineering Unit, Queen's University, Kingston,
Ontario, K7L 3N6, Canada
E-mail: loeb@biomed.queensu.ca, Fax: +1-613-545-6802

[1] *Present address:*
Department of Oral Anatomy (2nd division), School of Dentistry,
Hiroshima University, Hiroshima 734, Japan

Introduction

Although skeletal muscle motor units are often classified as being either slow-twitch or fast-twitch, it is well known that there exists a wide spectrum of contractile properties within these two classes (Burke 1981). Despite this fact, a common approach to modeling skeletal muscle is to assume that all slow-twitch motor units and all fast-twitch motor units are homogeneous. The properties of the whole muscle are then represented as a linear combination of a pure slow-twitch muscle in parallel with a pure fast-twitch muscle (Zajac 1989; Brown et al. 1996b). This approach is taken as a simple first-order approximation to avoid the unduly complex models that would result if each individual motor unit were modeled separately.

Data for such a model can be collected using either whole-muscle preparations, single motor units within a whole muscle, or single fibers. A drawback of both the single motor unit and single-fiber approaches is that the functional properties of a single motor unit or fiber are not necessarily representative of the population as a

whole. In contrast, a whole-muscle preparation composed exclusively of either slow-twitch or fast-twitch motor units can provide a representative combination of these properties. The 100% slow-twitch feline soleus (SOL) preparation (Ariano et al. 1973) has been used specifically for this reason (Rack and Westbury 1969; Scott et al. 1996). A 100% fast-twitch preparation that could act as a counterpart to SOL has not yet been developed.

The ideal whole-muscle preparation for studying the functional properties of fast-twitch muscle must satisfy two criteria. The muscle should be composed exclusively of fast-twitch fibers and should possess a simple architecture with relatively little in-series elasticity. The importance of having little in-series elasticity in a whole-muscle preparation was made apparent by the work of Scott et al. (1996) on SOL, which has a very large in-series elasticity. Scott et al. demonstrated that the velocities and length changes imposed on the whole muscle were significantly different from the velocities and length changes observed at the fascicle. These effects of a large, in-series elasticity cannot be eliminated properly in postexperiment analysis, thus limiting the interpretation of experimental data from such muscles. We propose here that feline caudofemoralis (CF), a hip extensor/abductor, could fill the role of an ideal preparation in which to study the contractile properties of fast-twitch muscles, as it already has for the ultrastructure and biochemistry of fast-twitch fibers (Van Winkle and Schwartz 1978; Van Winkle et al. 1978). CF is composed exclusively of fast-twitch fibers (Ariano et al. 1973; Van Winkle and Schwartz 1978), and preliminary investigations had shown that it could be prepared with only minimal series elasticity.

The purpose of this study was to create an archive of basic information about CF. In other muscles, systematic studies of motor unit physiology have proceeded from a knowledge base that includes information about motor unit compartmentalization within the whole muscle (English and Weeks 1984; Weeks and English 1985; Armstrong et al. 1988; Thomson et al. 1991), morphometry and physiological range of motion of the muscle (Goslow et al. 1973; Brown et al. 1996a), electromyographic activity in awake, unanesthetized cats (Engberg and Lundberg 1969; Walmsley et al. 1978; Pratt et al. 1991), the location of motoneuron somata in the spinal cord (Romanes 1951; Burke et al. 1977; Gordon et al. 1991; Hoover and Durkovic 1991; Hörner and Kümmel 1993), the architecture and end-plate banding of the muscle (Loeb et al. 1987), and the mean innervation ratio ($\overline{IR}$) of its motor units (Burke and Tsairis 1973; Burke et al. 1974; McDonagh et al. 1980; Dum et al. 1982). We undertook to gather these data from CF so that future studies utilizing CF would have access to this knowledge base.

Materials and methods

All experiments were carried out on adult cats of either sex, following the guidelines of the Canadian Council on Animal Care, and were approved by the Queen's University Animal Care Committee. During surgery, animals were anesthetized with pentobarbital sodium (initial dose of 35 mg/kg, supplementary doses of 5 mg/kg) at levels sufficient to abolish the pedal withdrawal reflex. For acute experiments, a tracheal tube was inserted. For chronic experiments, an antibiotic (Penlong S, Rogan/ST; 0.5 ml i.m.) was administered 1 day prior to and on the day of surgery. Throughout all experiments, core body temperatures were maintained at 36–38°C with a heating blanket connected through a feedback circuit to a rectal probe. At the end of an experiment, animals were killed with an overdose of pentobarbital sodium administered intravenously. Where feasible, animals were used for more than one type of experiment.

Range of motion and CF dissection

CF range of motion (ROM) was measured on the left legs of one male (5.2 kg) and nine female (2.4–3.8 kg) cats. CF was exposed minimally, exposing only the superficial surface of CF, as well as the insertion tendon and aponeurosis. The extensor caudae lateralis muscles from the first three caudal vertebrae (Ca1–Ca3) were removed bilaterally, exposing the Ca2 transverse process from which CF originates on the ventral surface. CF muscle-belly length was determined by measuring the length of a suture laid on the superficial surface of the muscle from the dorsal surface of the Ca2 transverse process to the end of the most distal fiber. For very short muscle lengths, the tendon was pulled to remove any slack.

Four leg positions were identified according to three joint angles suggested by Goslow et al. (1973): ileofemoral angle, defined as the angle between the anterior iliac crest, greater trochanter, and lateral epicondyle (θ in Fig. 6); ischeofemoral angle, defined as the angle between the ischeal tuberosity, greater trochanter, and lateral epicondyle (not shown in Fig. 6); and knee angle, defined as the angle between the greater trochanter, lateral epicondyle, and lateral malleolus (ϕ in Fig. 6). Two leg positions were chosen to produce the minimum and maximum *in situ* muscle lengths (L_{min} and L_{max}). The third leg position was at an ischeofemoral angle of 80° and a knee angle of 110° to produce the muscle length L_{extend}, whereas the fourth leg position was at an ileofemoral angle of 95° and a knee angle of 100° to produce the muscle length L_{stand}. These last two sets of joint angles correspond approximately to the joint angles expected at the end of the extension phase for both walking and trotting and during quiet stance, respectively (Goslow et al. 1973).

Morphometry

At the beginning of the ROM experiments described above, thigh and shank lengths were measured. Thigh length was measured as the distance between the femur's greater trochanter and lateral epicondyle; shank length was measured as the distance between the femur's lateral epicondyle and the fibula's lateral malleolus (knee joint held at 90°). Following the ROM experiments, the animals were killed and allowed to rigor for 6–12 h. The ipsilateral muscle was excised and the aponeurosis lengths were measured at the origin and insertion. Samples were removed from at least three different regions of the muscle, mounted in glycerol on glass slides, and examined using light microscopy to measure sarcomere lengths. At least 20 counts of the number of sarcomeres in 58 μm were made. The highest and lowest counts were discarded and a mean rigored sarcomere length calculated from the remaining values. Sarcomere L_0 was defined as the sarcomere length at which maximal isometric tetanic force F_0 would occur as calculated from fascicle L_0, rigored fascicle length, and mean rigored sarcomere length. Because edema could have been produced in the ipsilateral muscle by exposure and work (Murphy and Beardsley 1974), the contralateral muscle was excised and weighed.

Histochemistry

CF muscles from two males (3.5 kg and 5.4 kg) and six females (2.1–3.8 kg) were excised immediately following death, cut into 10- to 20-mm-long blocks, and frozen in liquid nitrogen. To validate

our staining procedure, we also removed medial gastrocnemius (MG) muscles from two of the animals as controls. Cross sections 18 μm thick were cut on a cryostat at –18°C and mounted on gelatin-coated slides. Slides from four CF muscles were stained only for adenosine triphosphatase (ATPase) activity using an alkaline (pH 10.4) preincubation (Guth and Samaha 1969). Adjacent sections from the other four CF muscles were stained for ATPase activity and for nicotinamide adenine dinucleotide (NADH) diaphorase activity (following the method of Dubowitz and Brooke, 1973). To estimate the fiber-type composition of each CF muscle, at least 500 fibers were sampled randomly by type identifying all fibers in five to seven rectangular fields (300×400 μm each) according to differences in ATPase reactivity.

Preliminary results from sections stained for NADH activity suggested that the oxidative staining properties of type IIB fibers depended on the size of the fiber cross section. To quantify this observation, we digitized over 200 type-identified type IIB fibers from a single region on one section in two different animals (using the MCID M2 system by Imaging Resources). From these digital images, the mean single-fiber diameters were calculated and the relative optical densities of the NADH reactivities were recorded. Correlations between fiber diameter and optical density were computed independently for each animal.

Stimulation of CF

Because stimulation of CF was to be carried out through the ventral roots, we first denervated most of the hindlimb. Using an inguinal approach, the femoral nerve was ligated just distal to exiting iliopsoas, proximal to where it trifurcates. The obturator nerve was ligated on the deep, medial side of iliopsoas, just anterior to the femoral nerve ligature. The sciatic nerve was ligated as it passed beneath the deep surface of CF. The branch (or branches) of the inferior gluteal nerve innervating gluteus maximus (GMax) were cut.

CF was then dissected free from the surrounding tissue except on the deep surface near its origin where the blood supply and innervation enter. The animal was secured to an adjustable frame with vertebral clamps on L4 and S2 (as described previously by Scott et al. 1996). A third clamp was placed on Ca2 to stabilize the origin of the muscle. The insertion tendon was cut and clamped to a force transducer (described previously by Scott et al. 1996) at the point where the most distal muscle fascicles ended. A pool was made using flaps of skin in which warmed paraffin oil was poured to cover the muscle. The oil was kept warm at 36–38°C throughout the experiment by a thermostatically controlled heater in the pool. Two stranded stainless steel wires were inserted transversely through the muscle approximately 5 mm apart to record electromyographic M-waves.

A laminectomy from L5 to S1 was carried out to permit ligation and section of the L6, L7, and S1 dorsal and ventral roots as close to their exit from the spinal cord as possible. A second pool filled with paraffin oil was constructed to protect the exposed tissues and maintained at 35–39°C. The L6, L7, S1, and S2 ventral roots were stimulated in turn while monitoring M-wave activity to identify the roots that innervated CF. Each root was laid across bipolar platinum hook electrodes and stimulated with constant voltage, 0.2-ms-duration square pulses at ×5 threshold.

Once the roots innervating CF were identified, whole-muscle tetanic isometric force was measured at six or seven different lengths spaced 4 mm apart. Stimulus trains at 120 pps for 120 ms were chosen on the basis of pilot experiments that showed that this protocol reliably produced a maximal, stable force plateau with minimal fatigue. Care was taken to ensure that the lengths bracketed L_0 [optimal length producing maximal isometric force (F_0)]. Muscle length was changed by a computer-controlled, motorized puller to which the force transducer was attached in-series with the muscle (previously described by Scott et al. 1996). Previously constructed templates allowed the computer to control muscle length and stimulation while simultaneously recording force and a rectified, bin-integrated electromyogram (EMG; Bak and Loeb 1979) at 600 samples per second. To avoid potentiation and fatigue, 5-min passive intervals were inserted between tetanic trains.

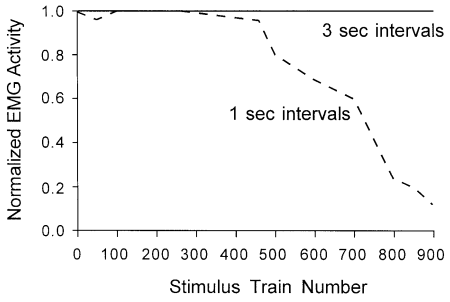

Fig. 1 Rectified, bin-integrated electromyogram (*EMG*) activity of caudofemoralis muscle (CF) during glycogen depletion protocols. EMG of the final pulse of a stimulus train (40 pps, 330 ms) was normalized to the peak level and plotted against stimulus train number. Stimulus trains were applied at either 3-s intervals (*solid line*; n=1) or 1-s intervals (*dashed line*; n=1). No statistics are presented because of the small n-value

Glycogen depletion and compartmentalization

Preliminary experiments were conducted to validate Burke's method of glycogen depletion (Burke et al. 1973) for CF. Stimulation was applied via a 6-mm bipolar nerve cuff (stranded stainless wires separated by 3 mm; described by Scott et al. 1996) to the inferior gluteal nerve proximal to branching into separate CF and GMax nerves. To avoid reflex activation, a ligature was tied around the inferior gluteal nerve proximal to the nerve cuff. We applied 40 pps trains for 330 ms at 1-s intervals for 15 min (Burke et al. 1973; n=2). Subsequent staining for glycogen using the method described below revealed that <60% of the fibers were fully depleted in both muscles. We then tested a modified depletion protocol on CF: 40-pps trains for 330 ms at 3-s intervals for 45 min (same number of stimulus trains as with Burke's method). Glycogen was observed to be depleted from all of the muscle fibers following this modified protocol (n=2).

In one of the muscles from each of the above protocols, we recorded rectified, bin-integrated EMG using the methods described above. To compare the effects of the two protocols, the level of EMG activity at the end of a stimulus train was plotted against stimulus train number in Fig. 1. We observed no change in the level of EMG activity when stimulus trains were applied at 3-s intervals, whereas we observed a large drop in EMG activity when stimulus trains were applied at 1-s intervals. These preliminary findings (n=1) suggest three possible mechanisms that might be responsible for the failure of Burke's method of glycogen depletion with CF: failure of the action potential to propagate along the motor axon, transmission failure at the neuromuscular junction, or failure of the action potential to propagate along the sarcolemma.

Preliminary examinations revealed that the CF nerve usually bifurcates just after entering CF. To evaluate the pattern of innervation in two cats (6.5 kg male and 2.2 kg female), we cut one of the two nerve branches and depleted the glycogen stores in the muscle fibers innervated by the other branch using the modified depletion protocol developed above. Immediately following the end of stimulation, the muscles were excised, cut into three or four blocks, and frozen on chucks in liquid nitrogen, recording the block orientation. Sections were cut on a cryostat as described above every 8–10 mm. The tissue was then stained using the periodic acid-Schiff's (PAS) procedure for the demonstration of glycogen (Drury and Wallington 1980). Stained sections were magnified using a microfilm reader. Fibers were identified as depleted if they showed a complete absence of PAS reactivity. The percentage of fibers depleted in various regions from each section was estimated by counting at least 200 randomly sampled fibers in each region.

Fatigue sensitivity

The fatigue sensitivity of CF was measured in two female cats (3.2 kg and 5.3 kg) by recording contractile force over time while a repetitive stimulus was applied to the CF nerve. A standard stimulus protocol for testing fatigue sensitivity has been developed by Burke et al. (1973) for MG (40 pps trains for 330 ms at 1-s intervals). This protocol was found to be inappropriate for CF glycogen depletion and so was also assumed to be inappropriate for testing CF fatigue sensitivity. Instead, we applied the modified glycogen depletion protocol described above for 1 or 2 h (40 pps trains for 330 ms at 3-s intervals). CF was isolated and attached to a force transducer. The incision was sutured shut leaving only a small hole through which the clamp could be inserted. The length of the muscle was adjusted to set its passive tension to 1.0 N. Peak force of contraction was recorded for every third contraction. The same experiment was repeated on MG in both animals to provide a comparison (passive tension for MG set to 10 N).

Electromyography

In two animals (one male, 4.1 kg; one female, 2.2 kg), chronic implants were used to record muscle activity during unanesthetized, conscious behaviors using methods described elsewhere (Hoffer et al. 1987). Briefly, bipolar, epimysial EMG "patch" electrodes consisting of two stranded stainless steel wires (3- or 5-mm spacing, depending on muscle size) were sutured onto the fascia surrounding a variety of hindlimb muscles under aseptic conditions. In one animal, two 3-mm patches were placed over different regions of CF (distal superficial surface and deep proximal surface) to evaluate the possibility that the neuromuscular compartments identified in the glycogen depletion experiments might be recruited differentially. The wires from each patch were passed subcutaneously and soldered to a 40-pin saddle connector that was attached to the lumbar vertebrae. Animals were trained to perform a variety of tasks including walking and trotting on a treadmill, ear-scratching, and paw-shaking. Signals from the EMG electrodes on CF and various other muscles and a time code were stored on magnetic tape for postexperiment synchronization with a videotape of the cat's behavior. EMG signals were then rectified, bin-integrated, and digitized at a rate of 150 samples/s.

Motor endplate staining

CF muscles from two female cats (2.6 kg and 3.0 kg) were excised under deep anesthesia and placed in acetylcholinesterase incubating medium (Lojda et al. 1979) for 8–12 h. The muscles were then rinsed in tap water and placed in a differentiating solution of 5% ammonium sulfide for 5 min. Following a second tap water rinse, the muscles were fixed in 10% formalin for 8–24 h and then stored in glycerol. Photographs of the muscles and their endplates were taken within 1 week of staining, because the stain deteriorates with prolonged storage.

Single-fiber microdissections

Whole CF muscles from three female cats (2.4–3.3 kg) were excised immediately prior to or following death and placed in 25% formic acid. The methods of acid digestion used here were similar to those used in previous studies (Loeb et al. 1987). Muscles were digested in 25% formic acid for 4–15 h, then stored in glycerol for between 2 weeks and 2.6 years. In all three cases the muscle tissue was still too tough for fiber dissection, so the muscles were digested further in 40% nitric acid for 1–2 h, and returned to more glycerol. The time spent in nitric acid for each muscle was determined by teasing muscle fibers every 10–20 min until fibers could be separated easily from each other. Dissections were found to become easier with prolonged storage in glycerol. Two muscles were additionally impregnated with gold chloride (1 h in 25% formic acid followed by 3–15 h in 1% gold chloride) prior to acid digestion to improve the visibility of individual fibers (Loeb and Gans 1986). Storage in glycerol included fresh changes of glycerol for each of the first 3–4 days. Muscles were rinsed briefly with distilled water between each of the steps.

Bundles of fibers 1–2 mm thick that extended the entire length of the muscle were dissected free and the bundle lengths were measured. Whole single fibers were then dissected carefully from these bundles. With practice and good tissue, almost all fibers could be dissected without breakage. The lengths of at least 50 complete fibers from each muscle were measured and expressed as a percentage of fascicle (bundle) length. During the dissection process (which took many hours over many days) the muscles and muscle bundles were stored in glycerol.

Retrograde labeling of motoneurons

Neuroanatomical experiments were carried out bilaterally on four adult female cats (1.9–3.2 kg). The CF and GMax nerves were isolated beneath the fascial plane separating the two muscles under aseptic conditions. Nerve identity was confirmed by stimulating the nerves and observing the location and extent of muscle contraction. Nerve branches were isolated for a length of at least 4–5 mm and were sectioned distally. All exposed tissue was covered with a layer of low-melting-point wax while gently holding the proximal nerve tips so that they protruded up through the wax. Small reservoirs were carved in the wax around the nerve tips and built up so that 1–3 mm of nerve tip could be exposed to solutions placed in the reservoir (see Gordon and Richmond 1990; Gordon et al. 1991 for details).

Prior to applying the fluorescent tracers, the reservoirs were filled with distilled water, left for 10 min and were then examined to ensure that no leakage occurred. The water was replaced with a drop of tracer solution and the reservoirs were sealed with wax. The tracers and concentrations used in this study included 10% Fluororuby (FR; dextran, tetramethylrhodamine, 3000 MW, anionic, lysine fixable; Molecular Probes), 6.6% Fluorogold (FG; hydroxystilbamidine; Fluorochrome), 3.3% Fast Blue (FB; proprietary compound; Sigma), and 10% fluoroscein-conjugated dextran (FD; Molecular Probes). In all cases, tracers were dissolved in 0.9% saline to which 2% dimethylsulfoxide was added (Huisman et al. 1982). After 2–3 h the wax overlying the pools was removed, tracer pools were inspected for leakage, and the tracer solutions were carefully blotted. The nerve tips were rinsed with saline and the rest of the wax was removed. The incisions were sutured and the cats allowed to recover for either 1 or 2 weeks.

At the end of the survival period, cats were reanesthetized deeply with pentobarbital sodium. CF muscles were removed for subsequent analysis followed by whole-body perfusion. Two liters of saline were perfused followed by 1.5 l of fixative (4% paraformaldehyde in 0.1 M acetate buffer, pH 6.5). The lumbosacral spinal cord from L5 to S3 was removed and fiduciary marks were placed at segmental boundaries. The spinal cord was transferred through a series of graded sucrose concentrations (10%, 20%, and 30%) in the same fixative over a 3-day period. The spinal cord was sectioned either longitudinally or transversely into 68-μm-thick sections. Sections were mounted onto gelatin-coated slides and coverslipped with DPX mounting medium.

The slides were examined using epifluorescent illumination. Three Leica filter blocks were used to identify cells labeled with fluorescent tracers: the A filter for FB and FG (BP 340–380 nm, LP 430 nm), the I2/3 filter for FD (BP 450–490 nm, LP 515 nm), and the N2.1 filter for FR (BP 515–560 nm, LP 580 nm). The positions and soma outlines of labeled cells were mapped using a camera lucida attachment on the microscope. Cells labeled with FR and FB were counted only if a nucleus could be identified. Occasionally the nuclei of FG-labeled cells were not easily distinguishable and so the criteria for identifying an FG-labeled cell were relaxed to permit inclusion in the counts if at least two dendrites could be identified. Traced soma outlines were later digitized and their areas calculated using specialized software (Optimas 4.01 by Bioscan).

Calculation of innervation ratio

The $\overline{IR}$ for each muscle was defined as the mean number of single muscle fibers per α-motoneuron and calculated by dividing the estimated number of muscle fibers by the number of labeled α-motoneurons. The total number of fibers in a muscle was estimated as the mean number of fibers per fascicle length (as determined from the single-fiber dissections described above) multiplied by the mean number of fibers per cross section. To estimate the number of fibers per muscle cross section, we used CF muscles from the animals used in the motoneuron-labeling study. CF muscles were excised and frozen in isopentane cooled with liquid nitrogen. The muscles were then removed from the isopentane, cut into three or four blocks, mounted, and then refrozen in liquid nitrogen. Sections were cut on a cryostat as described above and stained with hematoxylin and eosin.

Estimates of the mean number of fibers per cross section were made for six or seven cross sections evenly spaced along the length of each muscle. Sections were magnified and traced using a microfilm reader. The outlines were then digitized to calculate whole-muscle cross sectional area (Optimas 4.01 software by Bioscan). The estimated number of fibers per unit cross sectional area was calculated by counting the number of fibers in five to seven 300×400-μm regions from each section (minimum 500 fibers per section). The estimated number of fibers per cross section was calculated by multiplying whole-muscle cross sectional area times the number of fibers per unit cross sectional area.

Results

Histochemistry

The eight CF muscles that were examined histochemically were composed almost exclusively of type II fibers. Two muscles (one from a male cat, the other from a female cat) contained a small proportion of type I fibers (2 and 5%), whereas the other six muscles had none. The mean (±SD) composition of type IIA and type IIB fibers was 2±2% and 95±2%, respectively (n=8). Surprisingly, cross sections of type IIB fibers with large diameters stained more lightly for NADH than cross sections with small diameters (Fig. 2). To examine this feature more carefully, type IIB fibers identified by ATPase reactivity were identified in adjacent NADH-stained sections and quantified according to optical density and fiber diameter. The scatter plot of these two variables for 200+ fibers (Fig. 3) shows a significant correlation between optical density and fiber diameter (correlation calculated independently for each animal; in both cases $r>0.88$, $P<0.0001$).

Fig. 2A Photomicrograph of CF cross section stained for ATPase activity (preincubation at pH 10.4). This CF muscle was unusual because it contained a small proportion of type I fibers (*I*). Examples of each fiber type are marked. **B** Photomicrograph of a predominantly type IIB CF muscle stained for ATPase activity. **C, D** Photomicrographs of adjacent cross sections. The section shown in **C** was stained for ATPase activity; the section shown in **D** was stained for NADH diaphorase activity. *Dashed arrows* in each photomicrograph point to type IIA fibers; *solid arrows* point to examples of type IIB fibers that stained darkly for NADH diaphorase activity (note the small diameters of these darkly stained fibers). We believe that the small profiles are the narrowing, tapered ends of typical fibers (see Fig. 3). *Scale bars* 100 μm

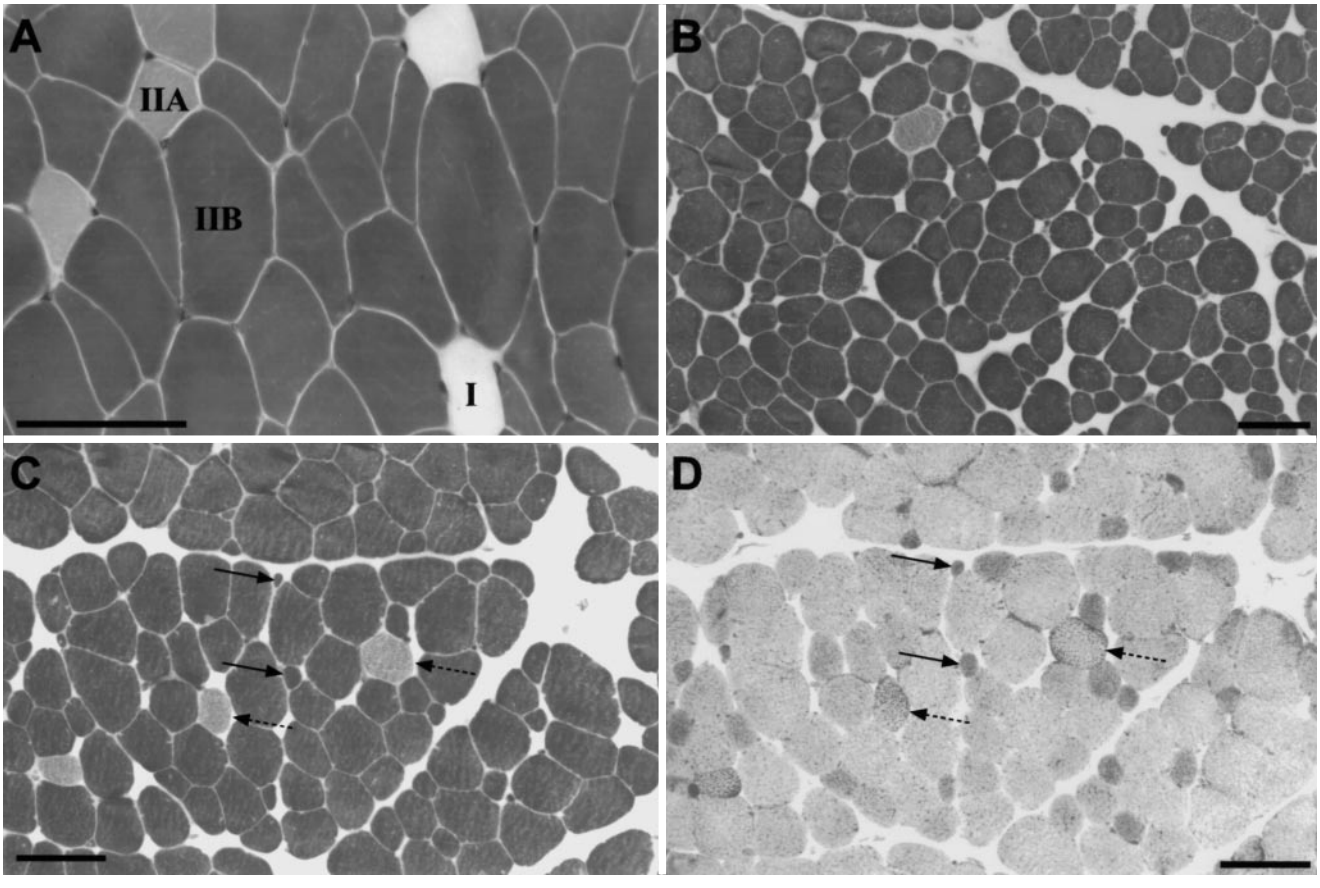

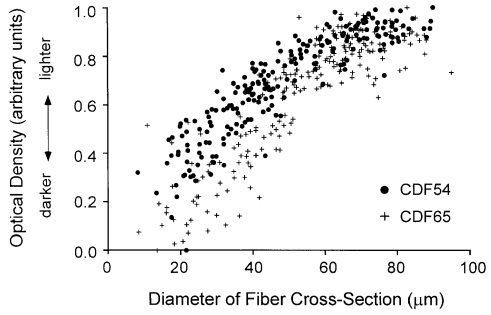

Fig. 3 Optical density plotted with respect to the diameter of individual CF fibers from a single cross section stained for NADH diaphorase activity for each of two animals (muscles CDF54 and CDF65; see Fig. 2 for example of staining pattern). Small fiber diameters presumably represent the narrowing, tapered ends of typical fibers. Optical density was measured on a linear scale in arbitrary units scaled between the darkest and lightest fiber for each cat. Optical density was linearly correlated with cross section diameter ($r>0.88$, $P<0.0001$, $n>200$)

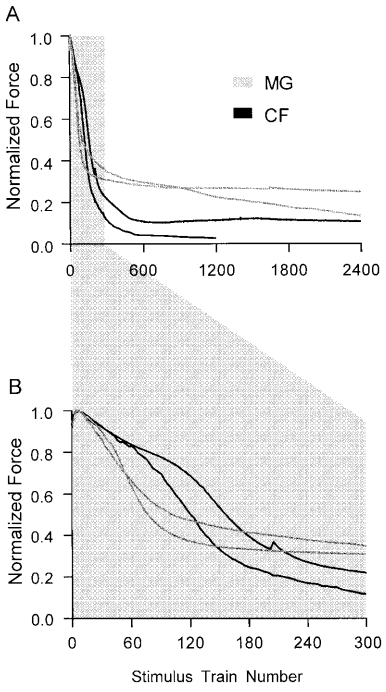

Fig. 4A, B Normalized peak force of contraction plotted against stimulus number for both CF and medial gastrocnemius (*MG*) during a modified version of Burke's fatigue test (40 pps, 330-ms-stimulus train applied every 3 s; Burke et al. 1973). **A** Force records during entire fatigue test. **B** Force records during the first 300 stimulus trains. CF force at train number 60 was significantly higher than MG force (Student *t*-test, $P<0.01$, $n=2$)

Fatigue sensitivity

When we applied our fatiguing protocol to MG, which is ~60% type IIB (Ariano et al. 1973; Burke and Tsairis 1973), we observed a large, rapid decline in force to a baseline level of 25–30% (Fig. 4). When our fatiguing protocol was applied to CF, which is ~95% type IIB (Ariano et al. 1973; Fig. 2), we observed a large, rapid decline in force to a baseline level of ~10% (Fig. 4). Surprisingly, the initial rate of force decline for MG was faster than for CF. A comparison of contractile force after 60 stimulus trains revealed that CF was producing significantly greater relative force than MG (Student *t*-test, $P<0.01$, $n=2$). Given that almost all of the early decline in MG force can be attributed to type IIB fibers (Burke et al. 1973), this early difference suggests that within CF and MG the fatigue sensitivity of the type IIB fibers may differ.

Electromyography

EMG activities recorded from one of the two cats are shown in Fig. 5. This figure shows the rectified, bin-integrated EMG from six different ipsilateral hindlimb muscles recorded during a pacing walk (a common gait in the treadmill; Blaszczyk and Loeb 1993). CF was active consistently during the stance phase of gait. The shape and timing of its EMG envelope was similar at the two CF sites (which correspond approximately to the two CF neuromuscular compartments described below) and qualitatively similar to that of GMax. Similar once-per-cycle activity patterns were observed for CF during normal walking, trotting, and paw-shaking behaviors (data not shown), as noted previously by Pratt et al. (1991). These patterns of recruitment were replicated in the second animal. CF was not observed to be active during ear scratching.

Morphometry

Various morphometric data for CF are summarized in Table 1. Because the one male cat was much larger than the female cats, his measurements are shown separately from the females. Linear regressions of CF L_0 and CF muscle mass with cat weight produced nonsignificant *r*-values of 0.45 and 0.50, respectively ($n=9$, $P>0.05$ for both), indicating that cat weight only accounts for about 20–25% of the variance in CF morphometry. Sarcomere L_0 was measured to be 2.5±0.2 μm in agreement with predictions from the sliding filament theory using feline myofilament lengths (Herzog et al. 1992). Physiological cross sectional area (PCSA) was defined by dividing muscle mass by muscle density (1.06 g/cm^3; Méndez and Keys 1960) and L_0. Specific tension (tension per unit cross sectional area) was calculated by dividing F_0 by PCSA. When the specific tensions of fast-twitch CF and slow-twitch SOL (as measured by Scott et al. 1996) were compared, no significant difference between them was found (31.2±4.7 N/cm^2 and 31.8±4.1 N/cm^2, respectively, mean ±SD; Student *t*-test, $P>0.8$).

Range of motion

CF acts primarily across the hip joint as both an extensor and abductor, but also has a small action at the knee as an

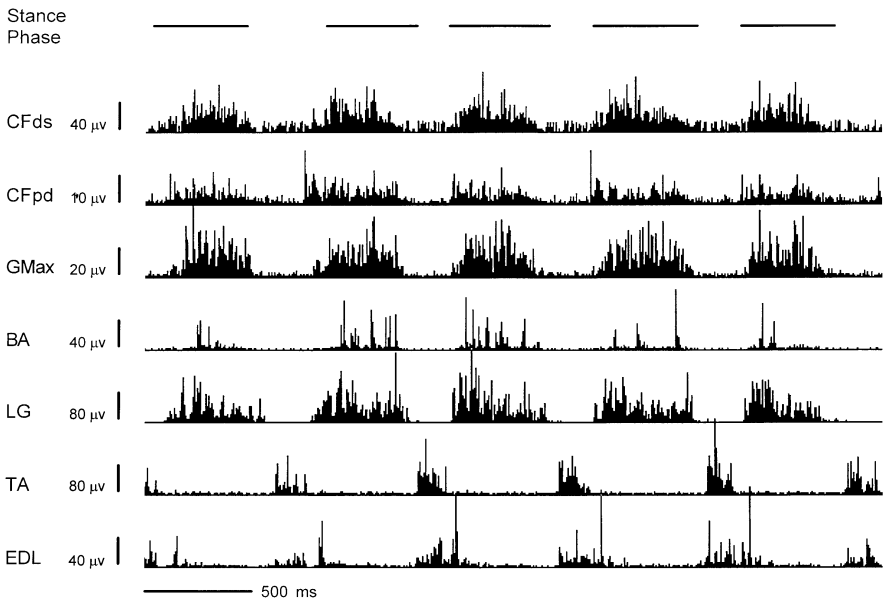

Fig. 5 Rectified, bin-integrated electromyogram activities of a variety of ipsilateral hindlimb muscles during pacing. The *top line* indicates duration of ipsilateral stance phase (*CFds* caudofemoralis, distal and superficial surface, *CFpd* caudofemoralis, proximal and deep surface, *GMax* gluteus maximus, *BA* biceps femoris anterior, *LG* lateral gastrocnemius, *TA* tibialis anterior, *EDL* extensor digitorum longus)

Table 1 Anatomical and physiological properties of feline caudofemoralis. Data are mean±standard deviation. These ten animals were also used for the range of motion data plotted in Fig. 6 (F_0 maximal, isometric, tetanic force, L_0 length at which F_0 occurs, *PCSA* physiological cross-sectional area)

Cats	9 females	1 male
Weight (kg)	3.3 ±0.4	5.2
Thigh length (cm)	9.7 ±0.3	11.2
Shank length (cm)	11.2 ±0.6	11.7
Muscle fascicle L_0 (cm)	5.6 ±0.6	5.7
Sarcomere L_0 (μm)	2.54±0.19	2.67
F_0 (N)	15.4 ±3.8	22.3
Muscle mass (g)	2.88±0.46	5.81
Origin aponeurosis (mm)	7.1 ±0.9	11.0
Insertion aponeurosis (mm)	17.2 ±3.2	20.0
PCSA (cm^2)	0.49±0.08	0.96
Specific tension (N/cm^2)	31.2 ±4.7	23.2

Correlations between cat weight and fascicle L_0 (r=0.45) and cat weight and muscle mass (r=0.50) were nonsignificant (n=9, $P>0.05$)

extensor. CF originates from the ventral surface of the Ca2 transverse process and inserts into the fascial complex attached to and surrounding the patella and joint capsule. The various joint angles and associated fascicle lengths that we measured are shown in Fig. 6 (the single male cat's measurements fell within the range observed for the females and so was included in the calculation of the means). The ischeofemoral angle was not reported, because it was found to be directly related to the ileofemoral angle (ischeal∠+ileal∠=210±5°). Muscle-belly lengths were converted to muscle-fascicle lengths by subtracting the mean aponeurosis length (one-half origin + one-half insertion aponeurosis). Changes in aponeurosis length due to compliance were ignored because of the relatively short aponeuroses (about one-fifth the length of the fascicles, Table 1). CF fascicle lengths were then normalized to L_0. The *in situ* ROM for CF was found to be from ∼0.6 to 1.2 L_0 (similar to the observation of Brown et al. 1996a). Although not explicitly shown here, changes in knee angle only affected fascicle length mildly, up to a maximum of 0.1 L_0 with extreme (140–150°) joint-angle changes. The angles we observed for L_{max} (ileofemoral and knee, 70° and 35°) are similar to the angles expected at the end of the flexion phase for both walking and trotting (ileofemoral and knee, 80° and 60–75°, respectively; Goslow et al. 1973). One can therefore estimate that the ROM of CF during walking and trotting is from ∼0.95 to 1.15 L_0.

Single fiber lengths

In total, 158 single fibers from three different muscles were dissected in this study. All fiber endings that ended intrafascicularly were observed to be tapered (see Loeb et al. 1987). A summary of fiber lengths, expressed as a percentage of muscle fascicle length, is presented as a histogram in Fig. 7 and also in Table 2. The histogram indicates a bimodal distribution with peaks at fiber length/fascicle length ratios of ∼0.33 and 0.45. Although the distribution was not Gaussian in nature, we performed an analysis of variance to compare the aggregate fiber lengths from the three muscles. The statistical results support acceptance of the null hypothesis that the three distributions came from the same population (F=0.56, $P>0.55$), suggesting that the distribution of CF fiber lengths (expressed as a percentage of fascicle length) is constant amongst female cats. The number of fibers per CF fascicle length was calculated from this aggregate population to be 2.26±0.05 (mean ±SE).

The scale for absolute fiber length included in Fig. 7 was calculated by assuming a fascicle L_0 of 5.6 cm (Table 1). Actual fiber lengths were not used because nitric acid digestion shrinks tissue substantially; in this study the shrinkage in muscle length was estimated at 30–50%. Us-

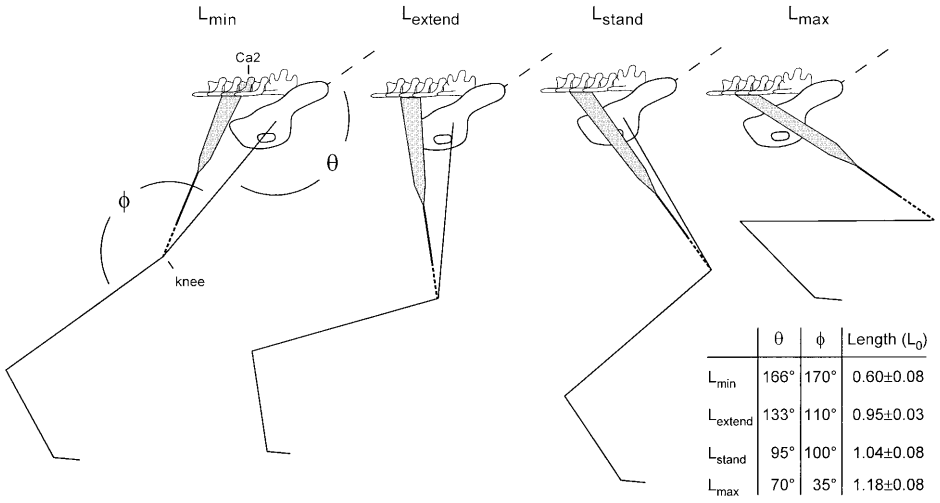

Fig. 6 CF fascicle lengths for four different leg positions (mean ±SD). θ and ϕ represent the ileofemoral and knee angles as defined by Goslow et al. (1973). SDs of all joint angles were 7° or less (n=5 for L_{extend} data, while n=10 for all others)

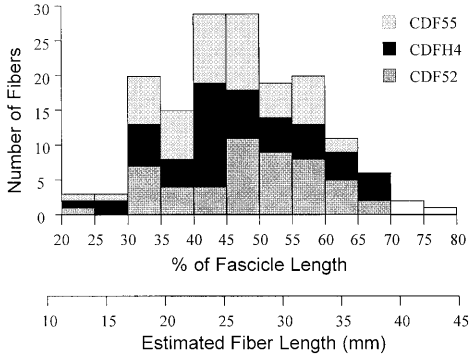

Fig. 7 Histogram of CF single-fiber lengths as a percentage of fascicle length. A second axis of "estimated fiber length" was obtained by using a muscle fascicle L_0 of 5.6 cm (Table 1). Single fibers were obtained through careful dissection of three CF muscles following acid digestion. The three distributions were not significantly different from each other (ANOVA, F=0.56, P>0.55)

ing a fascicle L_0 of 5.6 cm, the estimated minimum, mean, and maximum single-fiber lengths in CF are 1.1, 2.5, and 4.4 cm, respectively.

Motor endplate staining

CF muscles from two different animals were stained for acetylcholinesterase activity with similar results. The banding pattern of both muscles was similar and presumably corresponds to multiple endplate zones. Approximately four to six bands appear to cross any given fascicle extending the length of the muscle (see Fig. 8).

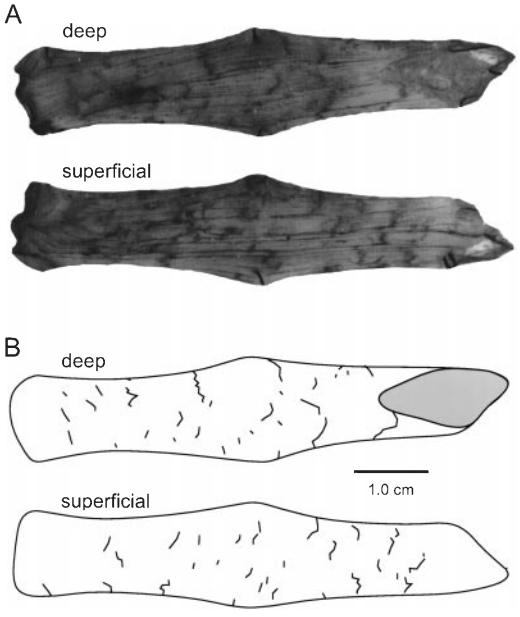

Fig. 8A, B Acetylcholinesterase stain of a single muscle viewed from both the deep and superficial surfaces. **A** Original photos of the muscle after staining. **B** Drawings of each surface with the endplates clearly marked

Compartmentalization

The CF nerve normally bifurcates just distal (2–5 mm) to its entry into the deep surface of CF. Rarely, however, this branching was observed to occur prior to nerve entry as shown in Fig. 9B. Figure 9A shows a reconstruction of one muscle in which the posterior nerve branch to CF

Table 2 Single-fiber lengths in caudofemoralis

	Muscle			
	CDF52	CDFH4	CDF55	Totals
Total fibers (n)	53	51	54	158
Double-tapered fibers (n)	9	11	16	36
Mean (±SD) ratio of fiber/fascicle length	0.44±0.13	0.46±0.11	0.43±0.12	0.44±0.12

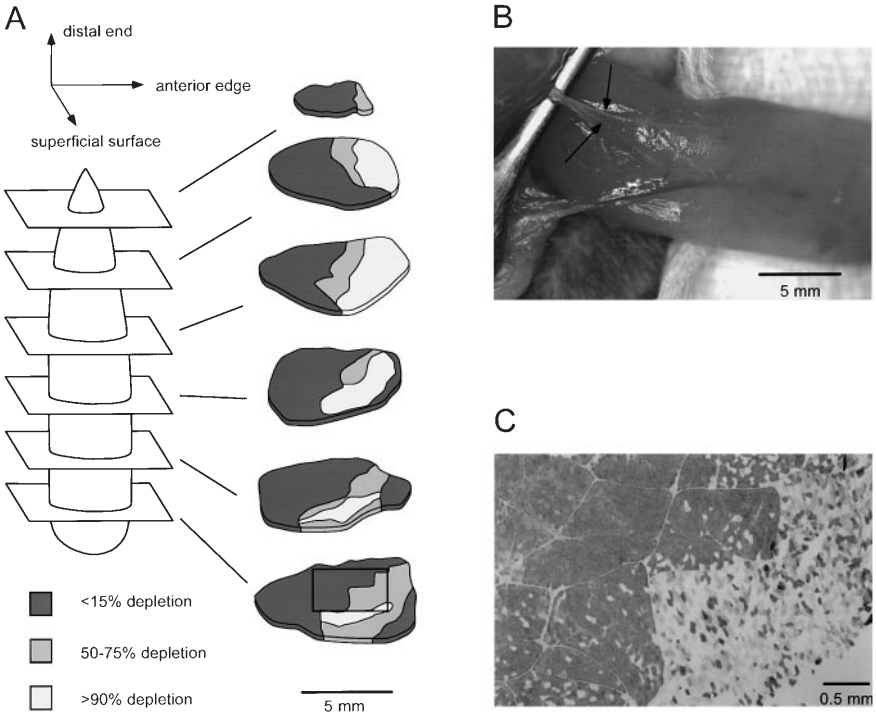

Fig. 9A Pattern of glycogen depletion (left CF muscle) after sectioning one of two nerve branches (anterior branch intact). Frozen cross sections were taken from six different regions and stained for glycogen (sample picture is shown **C**). All fibers were either fully depleted or clearly undepleted. Percentages refer to the percentage of fibers within a given region that were fully depleted. **B** Example of CF nerve bifurcating prior to muscle entry (left muscle, deep surface). **C** Photomicrograph of a section stained for glycogen content (PAS stain) from the most proximal section in **A**. Light fibers are glycogen-free, whereas dark fibers contain glycogen

was cut and the remaining branch stimulated to deplete the glycogen in the innervated motor units. Three distinct regions extending the length of the muscle were observed according to variations in the percentage of depleted fibers. Regions of less than 15% depletion, 50–75% depletion, and more than 90% were all observed. The distinctive nature of these long, strip-like sub-volumes is demonstrated in a photomicrograph (Fig. 9C) which shows a portion of the most proximal cross section from this muscle. Similar qualitative data was obtained in a second muscle, also consistent with motor-unit regionalization.

Ventral root innervation

Results obtained from a prior series of experiments (Brown and Loeb 1998) using identical methods to those described here were grouped with the results of this study so that the ventral roots innervating CF could be identified in a total of 21 animals. In 2 animals, only the L7 root innervated CF, in 1 animal only the S1 root innervated CF, whereas in the remaining 18 animals (including the lone male) both the L7 and S1 ventral roots innervated CF.

Motoneuron organization and size

Motoneurons supplying CF and GMax were labeled in four animals. Typical examples of FG-, FB-, and FR-labeled cells are shown in Fig. 10. The staining characteristics of these tracers were essentially identical to those described previously (Liinamaa et al. 1997). Counts of labeled motoneurons are summarized in Table 3. In five of the eight CF motor nuclei, more than 100 labeled motoneurons were observed, four of which contained between 100 and 115 cells. In the other three CF motor nuclei, fewer then 90 labeled cells were observed; two of these three motor nuclei were from one cat. The counts of GMax-labeled motoneurons were highly variable, in part reflecting the use of FB as a tracer for this muscle. Fewer than five cells were labeled in either of the first two cats (1-week survival; Table 3), presumably because the transport times of 1 week were too short for this slow-moving tracer (Bentivoglio et al. 1980). Motor nuclei contained 80–95 cells in three of four GMax nuclei in the second two cats (2-week survival; Table 3).

The location and extent of the motor nuclei were consistent from one side of the spinal cord to the other within each cat, but varied between animals in a manner predicted by patterns of ventral root innervation. CF motor nuclei ranged from 0.75 to just over 1 spinal segment in rostrocaudal length. Their rostral edges varied in location from rostral L7 to mid-L7. GMax motor nuclei ranged in rostrocaudal extent from 1 to 1.5 spinal segments, with a consistent rostral edge in mid-L6. A comparison between the relative locations of the CF and GMax motor nuclei within a given animal revealed extensive overlap. The rostrocaudal overlap was 1 full spinal segment in one animal (Fig. 10E) and 0.5 of a spinal segment in another animal (Fig. 11). In the transverse plane, the motor nuclei intermingled so extensively in both animals that they appeared to form a single column in the gray matter (Fig. 10D,E).

Two peaks were observed in the distribution of CF motoneuron diameters from the three motor nuclei containing the most labeled cells (Fig. 12). The smaller peak at 25–30 μm was assumed to represent γ-motoneurons,

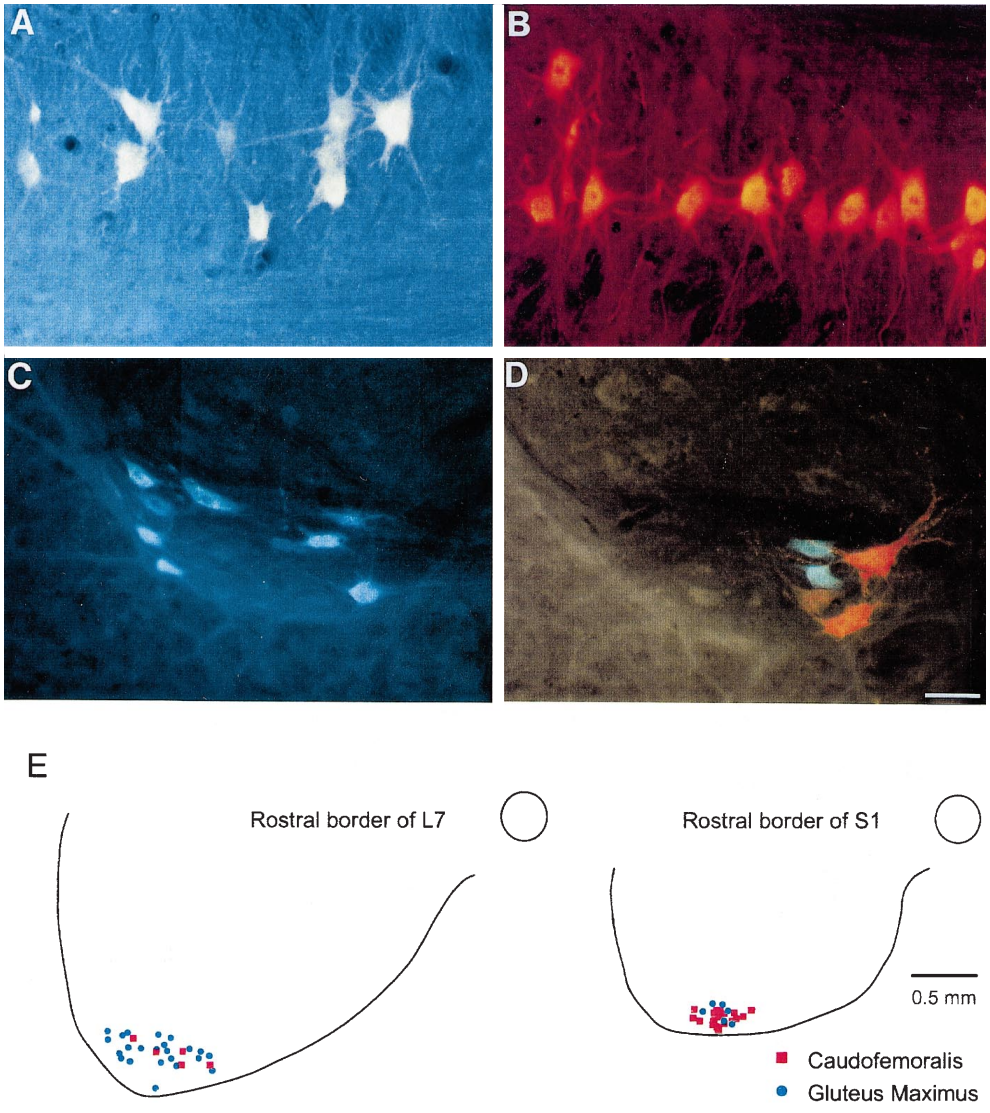

Fig. 10A–D Photomicrographs of motoneurons labeled with fluorescent tracers. **A** Fluorogold-labeled CF motoneurons (longitudinal section from animal CMN2). **B** Fluororuby-labeled CF motoneurons (longitudinal section from animal CMN2). **C** Fast blue-labeled GMax motoneurons (cross section through mid-L7 from animal CMN3). **D** Double exposure of Fluororuby-labeled CF motoneurons and fast blue-labeled GMax motoneurons (cross section through mid-L7 from animal CMN3). **E** Transverse reconstructions of the ventral horn showing the distributions of labeled CF and GMax motoneurons (right side of spinal cord from animal CMN3). Each reconstruction represents 1 mm of tissue. The two reconstructions represent the rostral and caudal borders of the region where the CF and GMax motor nuclei overlap, corresponding approximately to rostral L7 and rostral S1. *Scale bar* 100 μm **A–D**

Table 3 Labeled motoneuron counts (*FG* Fluorogold, *FR* Fluororuby, *FB* Fast Blue, *FD* fluoroscein-conjugated dextran)

Animal	Survival time (weeks)	Labeled CF motoneurons		Labeled GMax motoneurons	
		Left side	Right side	Left side	Right side
CMN1	1	85 (FG)	25 (FR)	0 (FB)	No dip
CMN2	1	108 (FG)	112 (FR)	No Dip	5 (FB & FD)
CMN3	2	88 (FR)	113 (FG)	91 (FB)	83 (FR)
CMN4	2	167 (FR)	102 (FG)	14 (FB)	83 (FR)

whereas the second, much larger peak at 50–55 μm was assumed to represent α-motoneurons. The minima between the two peaks (35 μm) was chosen as the cutoff diameter separating the γ-motoneurons from the α-motoneurons. Mean diameters of the CF γ- and α-motoneurons were 28±4 and 52±7 μm, respectively, (Table 4).

Mean innervation ratio

The $\overline{IR}$ was calculated for three CF muscles. Each muscle was from a different animal; in each case the muscle with the greater number of labeled motoneurons was chosen. The estimated number of fibers per cross section for these three muscles ranged from 10 600 to 16 100 (Table 4). These numbers were then multiplied by the previously calculated 2.26 fibers per fascicle length to estimate the total number of fibers in each of these muscles. These numbers (plus the number of α-motoneurons listed in Table 4) were then used to calculate the $\overline{IR}$ for each muscle (Table 4). The mean of the $\overline{IR}$s for the three CF muscles was ~270 and ranged from 253 to 309. In an attempt to quantify the accuracy of our calculations, we used 2% error in the number of fibers per fascicle length, estimated

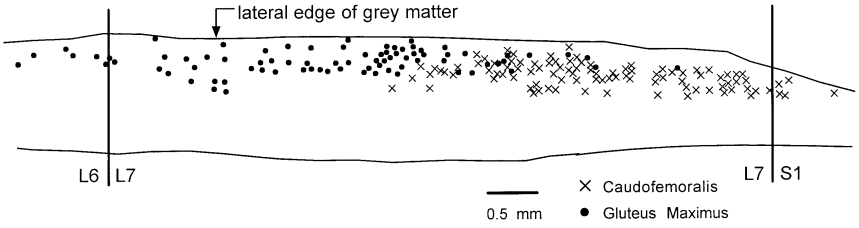

Fig. 11 Longitudinal reconstruction of the spinal gray matter showing the distributions of all labeled CF and GMax motoneurons (right side of spinal cord from animal CMN4)

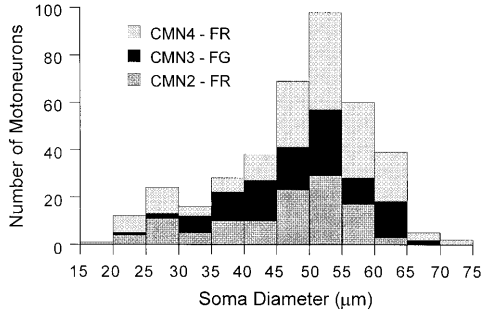

Fig. 12 Histogram of CF motoneuron soma diameters for three motor nuclei. Motoneuron somas were from longitudinal sections (animals CMN2, CMN4) or cross sections (animal CMN3). The minima between the two peaks (35 μm) was used as a cutoff diameter between α- and γ-motoneurons. No attempt was made to correct for possible tissue shrinkage (*FR* Fluororuby, *FG* Fluorogold)

Table 4 Motor innervation ratio. Cutoff diameter between γ- and α-motoneurons was estimated as 35 μm (see Fig. 12). Motor innervation ratio is defined as the mean number of fibers per α-motoneuron

	Cat		
	CMN2	CMN3	CMN4
γ-Motoneurons	20	10	23
Mean (±SD) diameter) (μm)	28±3	31±4	26±4
α-Motoneurons	92	103	144
Mean (±SD) diameter (μm)	50±6	51±8	54±7
Fibers per muscle cross section	10600	14100	16100
Mean motor innervation ratio	261	309	253

5% error from our fibers per cross section counts, and estimated 10% error in our motoneuron counts. Using standard error propagation techniques (for independent sources of error), we estimate the total error in our $\overline{IR}$ calculation for each of the animals to be ~11%.

Discussion

Muscle fiber properties

Within a given motor pool, the order of motor-unit recruitment tends to proceed according to fiber-type from slow-twitch, nonfatiguable units to fast-twitch, fatigue-resistant units, and finally to fast-twitch, fatiguable units (Burke 1981; Hoffer et al. 1987; Cope and Clark 1991; Tansey and Botterman 1996). Most muscles in the feline hindlimb are heterogeneous in fiber-type composition (Ariano et al. 1973). According to the recruitment-order hypothesis, most of these muscles will not recruit fast-twitch, fatiguable motor units during a low-intensity task such as walking (Engberg and Lundberg 1969; Walmsley et al. 1978; Pratt et al. 1991). In contrast, it appears that CF, composed almost exclusively of type IIB fibers, must recruit these fibers during walking; the absolute amplitudes of CF EMG were comparable with those of other locomotor muscles with mixed fiber types (Fig. 5; the bin integration analysis used in this study produces voltage calibrations approximately one-tenth of the peak-to-peak voltages of the raw EMG recordings; Bak and Loeb 1979). Regular use during locomotion probably explains why the type IIB fibers from CF appear to demonstrate a higher resistance to fatigue than the type IIB fibers from MG (Fig. 4). However, this raises the teleological question of why a muscle that is recruited in this manner would not have developed a greater proportion of type I and type IIA fibers. We suggest that some other property that is unique to type IIB fibers (e.g., very fast rise and fall times) may provide the answer to this question.

Another property that has been hypothesized to be fiber-type dependent is the relative force-producing capabilities of fast compared with slow-twitch muscle fibers (for an early review, see Close 1972). Most recent studies in cat have concluded that fast-twitch fibers develop significantly higher specific tensions (force per unit cross sectional area) than do slow-twitch fibers (Burke and Tsairis 1973; McDonagh et al. 1980; Dum et al. 1982; Bodine et al. 1987). In contrast, direct measurements by Lucas et al. (1987) on chemically skinned single fibers suggested that there was no significant difference between the specific tensions of different fiber types. In agreement with the findings of Lucas et al. we found no significant difference in the specific tensions produced by whole-muscle CF (exclusively fast-twitch) and whole-muscle SOL (exclusively slow-twitch; Scott et al. 1996). We suggest two possible reasons to explain these discrepancies. First, all but one of the previous studies (Bodine et al. 1987) used indirect measurements of specific tension, which we feel are likely to be less reliable than the direct measurements. Second, Bodine et al. (1987) based their study upon direct measurements of specific tension using single motor units within a whole muscle. Unfortunately, this technique has been shown recently to be problematic because of an artifact described by Heckman et al. (1992). Heckman et al. a depression in the isometric force of small motor units (i.e., slow-twitch) when a muscle was allowed to remain both isometric and quiescent for longer

than a few seconds. As a result, Bodine et al. (1987) may have underestimated the specific tensions for the small, slow-twitch motor units.

Although we have discussed motor unit recruitment order and specific tension in a manner that implies that fibers classified as one particular fiber-type are homogeneous, Burke (Burke et al. 1973; Burke 1981) has repeatedly stressed the importance of using fiber-type classifications as only a crude guide to motor unit properties, rather than as a rigid classification scheme. In this study we have observed three unexpected differences in the properties of type IIB fibers from CF as compared to type IIB fibers from MG. First, the glycogen depletion protocol developed by Burke et al. (1973) for MG does not successfully deplete CF (Fig. 1), presumably because some other part of the excitation-contraction process is failing first. Second, CF type IIB fibers appear to be less susceptible to fatigue than the MG type IIB fibers (Fig. 4). Third, we have observed a heterogeneity in the NADH staining intensity that depends upon fiber diameter (Figs. 2, 3). CF is composed of fibers that do not extend from one aponeurosis to the other; instead the fibers taper intrafascicularly. The darkly stained small diameters observed here appear to represent the narrowing, tapered ends of otherwise typically stained fibers. If true, then the differential NADH staining pattern we observed implies a nonuniform concentration of mitochondria over the length of a single fiber. Although we believe this staining pattern has not been reported before, it is not unique to CF; it can be seen also in feline sartorius muscle (SART; see Fig. 2 of Smits et al. 1994). The role, if any, of such a mitochondrial distribution is unknown. However, it may be related to other differences that exist in the tapered ends of fibers (e.g., myosin heavy-chain expression, presence of acetylcholinesterase) that in turn have been postulated to be important for longitudinal fiber growth (Rosser et al. 1995).

Series-fibered architecture

The pattern of tapered, intrafascicular fiber endings that we observed in CF is common for many feline hindlimb muscles whose fascicle lengths are greater than 3–4 cm (e.g., SART, tenuissimus, and semitendinosus; Loeb et al. 1987). A comparison of mean fiber length from the relatively short CF (L_0=5.6 cm, Table 1) to the relatively long SART or tenuissimus (L_0=9.2 cm and 14.5 cm, respectively; Brown et al. 1996a) revealed that the mean fiber length for all three muscles is approximately 2.5 cm (Loeb et al. 1987). It is not apparent why this similarity should exist in hindlimb muscles with varying architectures, when fibers from other feline muscles often have shorter mean fiber lengths (less than 2.0 cm, Richmond et al. 1985; Richmond and Armstrong 1988) and human leg muscles tend to have much longer mean fiber lengths (more than 10 cm, Heron and Richmond 1993).

A comparison of CF fiber length, expressed as a percentage of fascicle length, revealed a remarkable consistency between different specimens (Fig. 7, Table 2). The previously described relationship between the establishment of endplate bands and the growth of muscle fibers during development could explain this finding (Duxson et al. 1989; Duxson and Sheard 1995). The innervation zones of primary myotubes appear to be determined early in development. Secondary myotubes, which develop later into single fibers, grow around the innervation zones of primary myotubes in the developing animal. The arrangement of single fibers relative to the fascicle is thus predetermined during development by the innervation zones of the primary myotube, well before the final muscle size is determined.

Motor innervation

Retrograde tracers have provided a useful method by which to identify specific motor nuclei, but they do not always label cell populations with 100% effectiveness. The merits and problems associated with using the cut axon method have been discussed elsewhere (Haase and Hrycyshyn 1986; Richmond et al. 1994) and are not repeated here. To minimize the effects of any methodological problems, we applied different tracers on both sides of each animal. The tracers that we used to label CF motoneurons, FR and FG, were chosen because they are thought to be capable of labeling motor nuclei with 100% effectiveness under optimal conditions (Gordon and Richmond 1990; Kitamura and Richmond 1994). We also used FB in our study (only with GMax), because it has been shown previously to be effective at labeling α- and γ-motoneurons nonpreferentially, albeit with less overall efficacy (Gordon et al. 1991; Richmond et al. 1994). However, when an adequately long transport time was used for FB, we observed no consistent difference attributable to tracer type in the distributions, sizes, or numbers of labeled motoneurons.

It is unclear why we observed such a large range in CF motoneuron counts between animals (Table 3). Both FR and FB produced a similar distribution and number of labeled motoneurons to an HRP-labeled GMax motor nucleus labeled previously by Gordon et al. (1991), suggesting that our methods are technically sound. Interestingly, the wide variation in motoneuron number does not correlate with similar large variations in $\overline{IR}$ (Table 4). Furthermore, cat size (mass) did not account for much of the variability in CF morphometry such as muscle mass and fascicle L_0. We can only speculate that the mongrel cats used in our studies may have significant, quantitative interanimal variability of many neuromuscular elements related to genetic as well as behavioral idiosyncrastes. Fortunately, the qualitative architectural organization and physiological properties appear to be consistent across cats.

One of the benefits of the multitracer technique employed in the present study is that the locations of different motor nuclei can be compared directly. In correspondence to the anatomical locations of GMax and CF, the GMax motor nucleus was found rostral to the CF motor nucleus in the ventrolateral portion of the ventral horn

(Fig. 10). Furthermore, the observed location of the CF motor nuclei was consistent with the ventral root innervation patterns observed here. Rather than forming separate columns, however, the GMax and CF motor nuclei were found to intermingle extensively, and appeared to form part of a single column in the ventrolateral portion of the ventral horn; the location of this coextensive column was the same as that described by Romanes (1951) using degeneration techniques following section of the inferior gluteal nerve.

The substantial overlap of the CF and GMax motor nuclei is apparently an uncommon pattern. Almost all motor nuclei of muscles innervating the neck and shoulder region are anatomically separate (Hörner and Kümmel 1993; Kitamura and Richmond 1994; Liinamaa et al. 1997), as are many that innervate the hindlimb (Gordon et al. 1991; Hoover and Durkovic 1991). Overlap of MG and SOL motor nuclei (Burke et al. 1977) is one example that appears similar to the results observed here for CF and GMax. It is tempting to assign some measure of importance to this overlap, particularly in light of the similar patterns of activation for CF and GMax (Fig. 5). However, arguments that such arrangements may reflect a common embryological origin rather than a functional relationship between the two muscles have been presented previously (Hoover and Durkovic 1991; Hörner and Kümmel 1993; Liinamaa et al. 1997). If such is the case, the extensive overlap of the two motor nuclei might suggest that CF is a differentiated head of the gluteus muscle complex. Further work on developing animals is required before an adequate conclusion regarding this hypothesis can be made.

The two peaks that we observed in the distribution of CF soma size possibly reflect the presence of two separate populations of motoneurons: small-diameter γ-motoneurons and large-diameter α-motoneurons (Fig. 12). Assuming a cutoff diameter of 35 μm, γ-motoneurons comprise approximately 15% of the total population in CF. This percentage is significantly less than the 25–40% proportion of γ-motoneurons reported for other hindlimb muscles such as MG, flexor digitorum longus, lateral gastrocnemius, SART, SOL, and peroneus brevis (Burke et al. 1977; Dum et al. 1982; Weeks and English 1985, 1987; Gordon et al. 1991; Destombes et al. 1992). We have observed (I.E. Brown, T. Satoda, F.J.R. Richmond, G.E. Loeb, unpublished observations) that muscle spindles are distributed very sparsely in CF, as might be expected from the low proportion of γ-motoneurons. Previous studies have found that, in heterogeneous muscles, spindle densities tend to be lower in the fast-twitch regions than the slow-twitch regions (e.g. Richmond and Stuart 1985; Scott and Young 1987). If one considers CF to be a differentiated "head" of the gluteus complex, then the dearth of spindles in the fast-twitch CF would parallel the previous findings in single muscles with nonuniform distributions of fiber types.

By separating the γ- and α-motoneurons, we were able to calculate $\overline{IR}$ for CF. $\overline{IR}$ is often calculated by identifying all fibers belonging to a single motor unit and averaging the results from only a few motor units. In comparison, we indirectly estimated the $\overline{IR}$ for CF by dividing the total number of fibers for a single muscle by the total number of α-motoneurons belonging to that same muscle. The advantages of this second method include its simplicity, a true estimate of the mean (by including all motoneurons as opposed to a small sample), and the absence of sampling bias. Potential disadvantages of our method include no possible differentiation of $\overline{IR}$ for different fiber types within a single muscle, no indication of the range of innervation ratios for single motor units, and estimations (as opposed to direct counts) of both numbers used in the $\overline{IR}$ calculation (number of α-motoneurons and number of fibers). To minimize potential errors, we used large *n*-values in our fiber counts and chose the "best" labeled side from each animal for our motoneuron counts. The total random error in our calculations for each animal was estimated at ∼11%. Systematic undercounting of poorly labeled motoneurons would cause the true $\overline{IR}$ to be even lower than that reported here.

Table 5 Comparison of feline mean motor innervation ratios by fiber type. For studies that did not identify motor-unit types histochemically, the following equivalent motor-unit types were used (based upon Burke et al. 1973): slow nonfatiguable, *type I*; fast fatigue-resistant, *type IIA*; fast fatiguable, *type IIB*

Muscle	Fiber type		
	Type I	Type IIA	Type IIB
Soleus[a]	229	n.a.	n.a.
Medial gastrocnemius[b, c]	534, 611	440, 554	758, 674
Tibialis posterior[c]	393	363	491
Sartorius[d]	190	179	506
Biventer cervicus[e]	n.a.	408	408
Lateral gastrocnemius[f]	n.a.	n.a.	∼400
Flexor digitorum longus[c, g]	213, 180	125, 132	426, 328
Tibialis anterior[h]	93	197	255
Caudofemoralis	n.a.	n.a.	∼270

[a] Burke et al. (1974); [b] Burke and Tsairis (1973); [c] McDonagh et al. (1980); [d] Smits et al. (1994); [e] No differentiation between type IIA and type IIB fibers; Armstrong et al. (1988); [f] English and Weeks (1984); [g] Dum et al. (1982); [h] Bodine et al. (1987)

CF is composed almost exclusively of type IIB fibers. Assuming that type IIA and type I motor units in CF have smaller $\overline{IR}$s than type IIB motor units (see Table 5), we can estimate the $\overline{IR}$ for type IIB fibers in CF to be slightly greater than the whole-muscle $\overline{IR}$ of ∼270 (Table 4). We have compared estimates of $\overline{IR}$ for a number of other feline muscles with CF in Table 5. All but tibialis anterior have $\overline{IR}$s for type IIB motor units larger than CF. The $\overline{IR}$ for CF seems more typical of the estimates of $\overline{IR}$ for type IIA motor units (∼130–500, Table 5). The natural recruitment pattern of CF includes recruitment during repetitive behaviors such as walking and trotting (Fig. 5), patterns that are atypical of fast-twitch, fatiguable muscle, resembling more the patterns that are generally associated with type IIA or even type I motor units (Walmsley et al. 1978; Hoffer et al. 1987). The small $\overline{IR}$ for CF may be related to unusually frequent recruitment of its type IIB motor units, but it is not clear whether there is any causal link

between these properties or whether these results simply indicate a natural variation between different muscles.

Why study CF ?

Probably the most interesting feature of feline CF is that it is most often composed exclusively of fast-twitch fibers, which are almost exclusively type IIB (in agreement with the observations of Ariano et al. 1973 and Van Winkle and Schwartz 1978). Muscles such as CF have the advantage that they can be used as whole muscles to study properties unique to a particular fiber-type population. Examples of properties that are thought to be related to fiber type include recruitment via somatosensory reflexes (reviewed by Burke 1981), ultrastructure (Van Winkle and Schwartz 1978), specific tension, natural patterns of recruitment, mean innervation ratio, and posttetanic potentiation (Standaert 1964; Brown and Loeb 1998).

The methods used to examine CF in this study revealed a number of surprising observations that need further work to clarify and understand:

1. CF was surprisingly resistant to fatigue for a muscle composed primarily of type IIB fibers (Fig. 4).
2. The pattern of recruitment of CF during repetitive tasks such as walking was unexpected (Fig. 5).
3. The $\overline{IR}$ for type IIB fibers was low compared with that observed in most other feline hindlimb muscles (Table 5).
4. The small, tapering ends of type IIB single fibers stained more strongly for NADH diaphorase than the larger-diameter middle portions of type IIB fibers (Figs. 2, 3), possibly reflecting a differential mitochondrial density along the length of the fiber.
5. Burke's method of glycogen depletion failed to work on CF, with preliminary results suggesting that failure at the neuromuscular junction might be the cause (Fig. 1).
6. The overlap of the CF and GMax motor nuclei (Figs. 10, 11) and small number of γ-motoneurons in CF (Fig. 12, Table 4) are consistent with CF perhaps being a differentiated head of GMax.

It remains to be seen how many of these unexpected findings are interrelated, and it would be of particular interest to compare these findings to other feline muscles that are known to be nearly or completely 100% fast-twitch, including tensor fascia latae, sternomastoideus, and clavotrapezius (Ariano et al. 1973; Richmond and Vidal 1988).

For the purposes of recording the contractile characteristics of fast-twitch muscle, CF has a number of advantages over these other exclusively fast-twitch muscles. CF has a much simpler architecture, is parallel-fibered (nonpinnate), possesses two very short aponeuroses (Table 1), and has virtually no tendon at its origin. Thus an isometric contraction of CF prepared in the manner described in the present study is essentially isometric because the fascicle length remains constant during activation. This effect can be contrasted to a whole-muscle isometric contraction in SOL, which has significant shortening of the fascicles at the expense of the connective tissue [∼2:1 ratio of connective tissue to fascicle length (Scott et al. 1996) as compared to ∼0.2:1 ratio for CF (Table 1)].

In addition to its simple architecture, the gross innervation of CF suggests that its motor units work in parallel rather than in series (Fig. 9). This finding was consistent with the findings that different regions within CF had essentially identical patterns of activation during various behaviors (Fig. 5). Single fibers in CF do not run from end to end, but rather taper intrafascicularly (Table 2, Fig. 7). Thus, it is likely that a relatively even pattern of activation depends upon a more-or-less even distribution of single motor-unit fibers over the length of the muscle. Some other muscles organize their motor units both in parallel and in series (e.g., feline SART; Thomson et al. 1991). Activation of motor-unit populations that are arranged in series can result in a nonlinear summation of the forces from each of the populations (Scott et al. 1992). This problem is avoided when the motor-unit populations are arranged exclusively in parallel. The in-parallel organization of CF therefore permits us to conduct studies requiring asynchronous stimulation of split ventral roots to replicate physiological patterns of activation (as was done with SOL by Rack and Westbury, 1969). The combination of all of these properties in one muscle makes feline CF an ideal muscle in which to study the contractile characteristics of fast-twitch muscle.

Acknowledgements The authors would like to thank Lloyd Kennedy for help with using the MCID system and Janet Creasy, Kim Moore, Jennifer Conway, and Dave Kim for technical help with the experiments. This study was funded by the Medical Research Council of Canada.

References

Ariano MA, Armstrong RB, Edgerton VR (1973) Hindlimb muscle fiber populations of five mammals. J Histochem Cytochem 21: 51–55

Armstrong RB, Rose PK, Vanner S, Bakker GJ, Richmond FJR (1988) Compartmentalization of motor units in the cat neck muscle, biventer cervicis. J Neurophysiol 60: 30–45

Bak MJ, Loeb GE (1979) A pulsed integrator for EMG analysis. Electroencephalogr Clin Neurophysiol 47: 738–741

Bentivoglio M, Kuypers HG, Catsman-Berrevoets CE, Loewe H, Dann O (1980) Two new fluorescent retrograde neuronal tracers which are transported over long distances. Neurosci Lett 18: 25–30

Blaszczyk JW, Loeb GE (1993) Why cats pace on the treadmill. Physiol Behav 53: 501–507

Bodine SC, Roy RR, Eldred E, Edgerton VR (1987) Maximal force as a function of anatomical features of motor units in the cat tibialis anterior. J Neurophysiol 57: 1730–1745

Brown IE, Loeb GE (1998) Post-activation potentiation – a clue for simplifying models of muscle dynamics. Am Zool 38: (in press)

Brown IE, Liinamaa TL, Loeb GE (1996a) Relationships between range of motion, L_o and passive force in five strap-like muscles of the feline hindlimb. J Morphol 230: 69–77

Brown IE, Scott SH, Loeb GE (1996b) Mechanics of feline soleus. II. Design and validation of a mathematical model. J Muscle Res Cell Motil 17: 219–232

Burke RE (1981) Motor units: anatomy, physiology, and functional organization. In: Brooks VB (ed) Motor control (Handbook of physiology, sect 1, The nervous system). Am Physiol Soc, Bethesda, Md, pp 345–422

Burke RE, Tsairis P (1973) Anatomy and innervation ratios in motor units of cat gastrocnemius. J Physiol (Lond) 234: 749–765

Burke RE, Levine DN, Tsairis P, Zajac FE (1973) Physiological types and histochemical profiles in motor units of the cat gastrocnemius. J Physiol (Lond) 234: 723–748

Burke RE, Levine DN, Salcman M, Tsairis P (1974) Motor units in cat soleus muscle: physiological, histochemical and morphological characteristics. J Physiol (Lond) 238: 503–514

Burke RE, Strick PL, Kanda K, Kim CC, Walmsley B (1977) Anatomy of medial gastrocnemius and soleus motor nuclei in cat spinal cord. J Neurophysiol 40: 667–680

Close RI (1972) Dynamic properties of mammalian skeletal muscles. Physiol Rev 52: 129–197

Cope TC, Clark BD (1991) Motor-unit recruitment in the decerebrate cat: several unit properties are equally good predictors of order. J Neurophysiol 66: 1127–1138

Destombes J, Horcholle-Bossavit G, Thiesson D, Jami L (1992) Alpha and gamma motoneurons in the peroneal nuclei of the cat spinal cord: an ultrastructural study. J Comp Neurol 317: 79–90

Drury RAB, Wallington EA (1980) Carleton's histological technique. Oxford University Press, Oxford, pp 45–46, 360–362

Dubowitz V, Brooke MH (1973) Histological and histochemical stains and reactions. In: Walton JN (ed) Muscle biopsy: a modern approach. Saunders, London, pp 20–33

Dum RP, Burke RE, O'Donovan MJ, Toop J, Hodgson JA (1982) Motor-unit organization in flexor digitorum longus muscle of the cat. J Neurophysiol 47: 1108–1125

Duxson MJ, Sheard PW (1995) Formation of new myotubes occurs exclusively at the multiple innervation zones of an embryonic large muscle. Dev Dynam 204: 391–405

Duxson MJ, Usson Y, Harris AJ (1989) The origin of secondary myotubes in mammalian skeletal muscles: ultrastructural studies. Development 107: 743–750

Engberg I, Lundberg A (1969) An electromyographic analysis of muscular activity in the hindlimb of the cat during unrestrained locomotion. Acta Physiol Scand 75: 614–630

English AW, Weeks OI (1984) Compartmentalization of single muscle units in cat lateral gastrocnemius. Exp Brain Res 56: 361–368

Gordon DC, Richmond FJR (1990) Topography in the phrenic motoneuron nucleus demonstrated by retrograde multiple-labelling techniques. J Comp Neurol 292: 424–434

Gordon DC, Loeb GE, Richmond FJR (1991) Distribution of motoneurons supplying cat sartorius and tensor fasciae latae, demonstrated by retrograde multiple-labelling methods. J Comp Neurol 304: 357–372

Goslow GEJ, Reinking RM, Stuart DG (1973) The cat step cycle: hindlimb joint angles and muscle lengths during unrestrained locomotion. J Morphol 141: 1–41

Guth L, Samaha FJ (1969) Qualitative differences between actomyosin ATPase of slow and fast mammalian muscle. Exp Neurol 25: 138–152

Haase P, Hrycyshyn AW (1986) On the diffusion of horseradish peroxidase into muscles and the "spurious" labeling of motoneurons. Exp Neurol 91: 399–403

Heckman CJ, Weytjens JLF, Loeb GE (1992) Effect of velocity and mechanical history on the forces of motor units in the cat medial gastrocnemius muscle. J Neurophysiol 68: 1503–1515

Heron MI, Richmond FJR (1993) In-series fiber architecture in long human muscles. J Morphol 216: 35–45

Herzog W, Kamal S, Clarke HD (1992) Myofilament lengths of cat skeletal muscle: theoretical considerations and functional implications. J Biomech 25: 945–948

Hoffer JA, Loeb GE, Marks WB, O'Donovan MJ, Pratt CA, Sugano N (1987) Cat hindlimb motoneurons during locomotion. I. Destination, axonal conduction velocity and recruitment threshold. J Neurophysiol 57: 510–529

Hoover JE, Durkovic RG (1991) Morphological relationships among extensor digitorum longus, tibialis anterior, and semitendinosus motor nuclei of the cat: an investigation employing the retrograde transport of multiple fluorescent tracers. J Comp Neurol 303: 255–266

Hörner M, Kümmel H (1993) Topographical representation of shoulder motor nuclei in the cat spinal cord as revealed by retrograde fluorochrome tracers. J Comp Neurol 335: 309–319

Huisman AM, Kuypers HG, Verburgh CA (1982) Differences in collateralization of the descending spinal pathways from red nucleus and other brain stem cell groups in cat and monkey. Prog Brain Res 57: 185–217

Kitamura S, Richmond FJR (1994) Distribution of motoneurons supplying dorsal and ventral suboccipital muscles in the feline neck [published erratum appears in J Comp Neurol 1994, 351(2):328]. J Comp Neurol 347: 25–35

Liinamaa TL, Keane J, Richmond FJR (1997) Distribution of motoneurons supplying feline neck muscles taking origin from the shoulder girdle. J Comp Neurol 377: 298–312

Loeb GE, Gans C (1986) Electromyography for experimentalists. University Chicago Press, Chicago

Loeb GE, Pratt CA, Chanaud CM, Richmond FJR (1987) Distribution and innervation of short, interdigitated muscle fibers in parallel-fibered muscles of the cat hindlimb. J Morphol 191: 1–15

Lojda Z, Grossrau R, Schiebler TH (1979) Enzyme Histochemistry – a laboratory manual. Springer, Berlin Heidelberg New York

Lucas SM, Ruff RL, Binder MD (1987) Specific tension measurements in single soleus and medial gastrocnemius muscle fibres of the cat. Exp Neurol 95: 142–154

McDonagh JC, Binder MD, Reinking RM, Stuart DG (1980) Commentary on muscle unit properties in cat hindlimb muscles. J Morphol 166: 217–230

Méndez J, Keyes A (1960) Density and composition of mammalian muscle. Metabolism 9: 184–188

Murphy RA, Beardsley AC (1974) Mechanical properties of the cat soleus muscle *in situ*. Am J Physiol 227: 1008–1013

Pratt CA, Chanaud CM, Loeb GE (1991) Functionally complex muscles of the cat hindlimb. IV. Intramuscular distribution of movement command signals and cutaneous reflexes in broad, bifunctional thigh muscles. Exp Brain Res 85: 281–299

Rack PMH, Westbury DR (1969) The effects of length and stimulus rate on tension in the isometric cat soleus muscle. J Physiol (Lond) 204: 443–460

Richmond FJR, Armstrong RB (1988) Fiber architecture and histochemistry in the cat neck muscle, biventer cervicis. J Neurophysiol 60: 46–59

Richmond FJR, Stuart DG (1985) Distribution of sensory receptors in the flexor carpi radialis muscle of the cat. J Morphol 183: 1–13

Richmond FJR, Vidal PP (1988) The motor system: Joints and muscles of the neck. In: Peterson BW, Richmond FJR (eds) Control of head movement. Oxford University Press, New York, pp 1–21

Richmond FJR, MacGillis DRR, Scott DA (1985) Muscle-fiber compartmentalization in cat splenius muscles. J Neurophysiol 53: 868–885

Richmond FJR, Gladdy R, Creasy JL, Kitamura S, Smits E, Thomson DB (1994) Efficacy of seven retrograde tracers, compared in mulitple-labelling studies of feline motoneurones. J Neurosci Methods 53: 35–46

Romanes GJ (1951) The motor cell columns of the lumbosacral spinal cord of the cat. J Comp Neurol 94: 313–364

Romanes GJ (1964) The motor pools of the spinal cord. Prog Brain Res 11: 93–119

Rosser BWC, Waldbillig DM, Lovo SD, Armstrong JD, Bandman E (1995) Myosin heavy chain expression within the tapered ends of skeletal muscle fibers. Anat Rec 242: 462–470

Scott JJ, Young H (1987) The number and distribution of muscle spindles and tendon organs in the peroneal muscles of the cat. J Anat 151: 143–155

Scott SH, Thomson DB, Richmond FJR, Loeb GE (1992) Neuromuscular organization of feline anterior sartorius: II. Intramuscular length changes and complex length-tension relationships during stimulation of individual nerve branches. J Morphol 213: 171–183

Scott SH, Brown IE, Loeb GE (1996) Mechanics of feline soleus. I. Effect of fascicle length and velocity on force output. J Muscle Res Cell Motil 17: 205–218

Smits E, Rose PK, Gordon T, Richmond FJR (1994) Organization of single motor units in feline sartorius. J Neurophysiol 72: 1885–1896

Standaert FG (1964) The mechanisms of post-tetanic potentiation in cat soleus and gastrocnemius muscles. J Gen Physiol 47: 987–1001

Tansey KE, Botterman BR (1996) Activation of type-identified motor units during centrally evoked contractions in the cat medial gastrocnemius muscle. I. Motor-unit recruitment. J Neurophysiol 75: 26–37

Thomson DB, Scott SH, Richmond FJR (1991) Neuromuscular organization of feline anterior sartorius: I. Asymmetric distribution of motor units. J Morphol 210: 147–162

Van Winkle WB, Schwartz A (1978) Morphological and biochemical correlates of skeletal muscle contractility in the cat. I. Histochemical and electron microscopic studies. J Cell Physiol 97: 99–120

Van Winkle WB, Entman ML, Bornet EP, Schwartz A (1978) Morphological and biochemical correlates of skeletal muscle contractility in the cat. II. Physiological and biochemical studies. J Cell Physiol 97: 121–136

Walmsley B, Hodgson JA, Burke RE (1978) Forces produced by medial gastrocnemius and soleus muscles during locomotion in freely moving cats. J Neurophysiol 41: 1203–1216

Weeks OI, English AW (1985) Compartmentalization of the cat lateral gastrocnemius motor nucleus. J Comp Neurol 235: 255–267

Weeks OI, English AW (1987) Cat triceps surae motor nuclei are organized topologically. Exp Neurol 96: 163–177

Zajac FE (1989) Muscle and tendon: properties, models, scaling and application to biomechanics and motor control. Crit Rev Biomed Eng 17: 359–411